

First Example of Ambipolar Naphthalene Diimide Exhibiting Room Temperature Columnar Phase

Paresh Kumar Behera,^a Kajal Yadav,^b Nandan Kumar,^a Ravindra Kumar Gupta,^a
D. S. Shankar Rao,^c Upendra Kumar Pandey*^b and Ammathnadu Sudhakar Achalkumar*^{a,d}

^aDepartment of Chemistry, Indian Institute of Technology Guwahati, Guwahati, 781039, Assam, India.

^bOrganic & Flexible Electronics Laboratory, Department of Electrical Engineering, School of Engineering, Shiv Nadar Institution of Eminence, Delhi NCR, India.

E-mail: upendra.pandey@snu.edu.in

^cCentre for Nano and Soft Matter Sciences, Arkavathi Campus, Survey No.7, Shivanapura, Dasanapura Hobli, Bengaluru – 562162, India.

^dCentre for Sustainable Polymers, Indian Institute of Technology Guwahati, Guwahati, 781039, Assam, India.

Email:achalkumar@iitg.ac.in

Supporting Information

Table of Contents

Serial Number	Contents	Page numbers
1	Materials and methods	S2-S3
2	Experimental Section	S3-S5
3	NMR Spectra	S6-S7
4	MALDI-TOF Mass spectra	S8
5	Thermal gravimetric analysis	S9
6	Polarizing Optical Microscopy	S9-S10
7	Differential scanning calorimetry	S10
8	X-ray diffraction studies	S11-S12
9	Photophysical properties	S12-S13
10	Electrochemical properties	S13-S14
11	DFT Studies	S14-S17
12	Charge Carrier Mobility Studies	S17-S19
13	References	S19-S20

1. Materials and methods

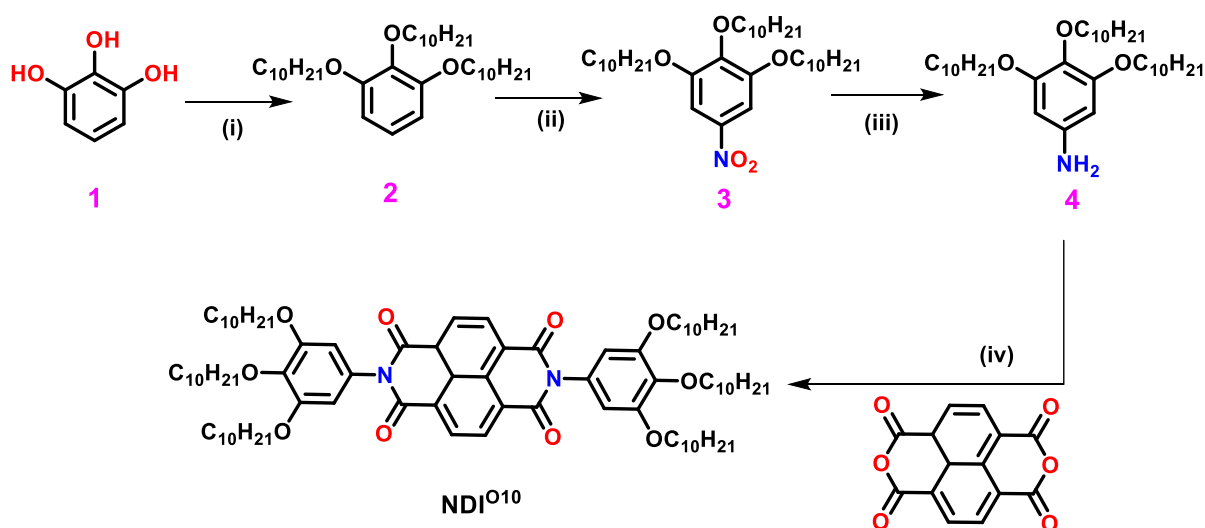
Commercially available chemicals were used without any purification; solvents were dried following the standard procedures. Chromatography was performed using either silica gel (60-120 mesh) or neutral aluminium oxide. For thin layer chromatography, aluminium sheets pre-coated with silica gel were employed. IR spectra were recorded on a Perkin Elmer IR spectrometer at normal temperature by using KBr pellet. The spectral positions are given in wave number (cm^{-1}) unit. NMR spectra were recorded using Bruker 600 MHz NMR spectrometer. For ^1H NMR spectra, the chemical shifts are reported in ppm relative to TMS as an internal standard. Coupling constants are given in Hz. Mass spectra were determined from MALDI-TOF mass spectrometer using α -Cyano-4-hydroxycinnamic acid as a matrix or High Resolution Mass Spectrometer. The mesogenic compounds were investigated for their liquid crystalline behavior (birefringence and fluidity) by employing a polarizing optical microscope (Nikon Eclipse LV100POL) equipped with a programmable hot stage (Mettler Toledo FP90). Clean glass slides and coverslips were employed for the polarizing optical microscopic observations. The transition temperatures and associated enthalpy changes were determined by differential scanning calorimeter (Mettler Toledo DSC1) under nitrogen atmosphere. Peak temperatures obtained in DSC corresponding to transitions were in agreement with the polarizing optical microscopic observations. The transition temperatures obtained from calorimetric measurements of the first heating and cooling cycles at a rate of $5\text{ }^\circ\text{C}/\text{min}$ are tabulated. Variable temperature X-ray diffraction measurements were carried out with samples filled in Lindemann capillaries. The apparatus essentially involved a high resolution X-ray powder diffractometer (PANalytical X'pert pro) with a high resolution fast detector PIXCEL. The temperature of the sample was varied using a Mettler hot stage/ programmer (FP82HT/FP90). Thermogravimetric analysis (TGA) was performed using thermogravimetric analyzer (Mettler Toledo, model TG/SDTA 851 e) under a nitrogen flow at a heating rate of $10\text{ }^\circ\text{C}/\text{min}$. UV-Vis spectra were obtained by using Perkin-Elmer Lambda 750, UV/VIS/NIR spectrometer. Fluorescence emission spectra in solution state were recorded with Horiba Fluoromax-4 fluorescence spectrophotometer or Perkin Elmer LS 50B spectrometer. Cyclic Voltammetry studies were carried out using a Versa Stat 3 (Princeton Applied Research) Electrochemical workstation.

For SCLC measurements, devices were fabricated in either electron-only (ITO/ZnO/NDIs/Ag) or hole-only (ITO/PEDOT: PSS/NDIs/MoO₃-Ag) architecture. In brief, pre patterned indium tin oxide (ITO) substrates (Xinyan Technologies, Taiwan, $15\ \Omega/\square$) were first cleaned using 3% soap solution in deionized water (Hellmanex III, Sigma-Aldrich) followed by cleaning with deionized water, acetone, and isopropyl alcohol for 20 minutes each sequentially in an ultrasonicator. The substrates were then gently blown dry with nitrogen gas and exposed to UV ozone treatment for 30 minutes at 50°C (BioBEE Tech, India) to remove any organic residues. For the fabrication of the hole only device (ITO/PEDOT: PSS/PBIs/MoO₃-Ag), a 40 nm PEDOT:PSS (Sigma Aldrich) layer was first spin coated at 4000 rpm for 65 seconds with a ramp rate of 2000 rpm followed by annealing of at $150\text{ }^\circ\text{C}$ on a hot plate for 20 minutes under ambient conditions. The active layer for both the NDIs was then spin coated on PEDOT: PSS at 1500 rpm for 45 seconds from a 10 mg/ml solution in

chloroform to achieve a thickness of 100 nm (measured using Dektak surface profilometer). Finally, a top contact of 7 nm of MoO₃ and 100 nm of Ag layer was sequentially thermally evaporated under high vacuum (2.2×10^{-6} mbar, Hind High Vacuum, India) to complete the devices. For, electron only device, a ZnO sol gel solution (200 mg zinc acetate dihydrate (Zn (CH₃COO)₂.2H₂O) + 52 mg ethanolamine in 2 mL 2-methoxy ethanol, agitated heavily overnight and filtered using 0.45 μm PTFE filter) was spin coated on cleaned ITO substrates obtain a thickness of ~30 nm (4500 rpm for 45 sec followed by annealing at 180 °C for 1 hour under ambient conditions). An active layer for both NDIs were then spin coated similar to what used for hole only devices. Finally, top contact of 100 nm Ag was evaporated at 2.2×10^{-6} mbar pressure for complete device. The active area of all devices was 0.066 cm² (measured through the overlap of ITO and top contact). Dielectric constant of NDIs was extracted from capacitance-voltage characteristics using high-frequency LCR meter ZM2376 (NF Corporation) with an applied oscillation level voltage of 1V and frequency sweep from 20 Hz to 2 MHz.

2. Experimental Section:

Scheme S1. Synthesis of NDI^{O10}



Reagents and conditions: (i) K₂CO₃, Dry DMF, C₁₀H₂₁Br, 80 °C, 12 h, 75% yield, (ii) NaNO₂, HNO₃, 0 °C, 1h, 86% yield, (iii) N₂H₄.H₂O, EtOH, H₂ -Pd/C, rt, overnight, 74% yield, (iv) Zn(OAc)₂, imidazole, microwave irradiation, 35 W, 35 min, 165 °C, 82%.

Compounds **2**,^[S1] **3**,^[S1] **4**,^[S2] **6**,^[S4] **7**,^[S5] **8**^[S5] were prepared as reported earlier. NDI^{O10} and NDI^{I0} were prepared by following the method used for the synthesis of perylene bisimides.^[S3]

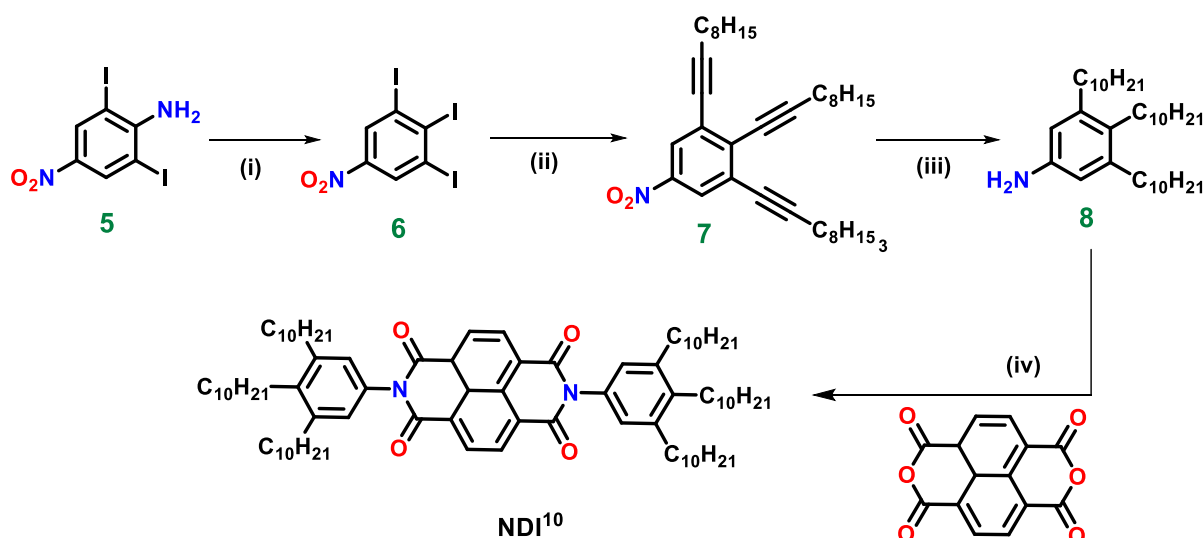
Procedure for synthesis of NDI^{O10} [S3]

Naphthalene-3,4,9,10-tetracarboxylic dianhydride (1 eq.), tridecyloxy aniline (2.2 eq.), zinc acetate (2 eq.) and imidazole (1 g) were taken in a microwave vessel, flushed with nitrogen and put in microwave reactor. The mixture was heated at 165 °C for 35 minutes at 35 W and 100 psi pressure. After cooling, reaction mixture was poured in 2(N) HCl (10 mL) and extracted

with chloroform. Organic mixture was washed with water and saturated sodium chloride solution. The crude compound was purified by neutral alumina column chromatography using 50% chloroform-hexane system. Further purification was done by recrystallization from chloroform-methanol system.

$R_f = 0.5$ (30% EtOAc-Hexane); Creamy brown solid, yield: 82%; IR (KBr pellet) ν_{\max} in cm^{-1} : 2921, 2852, 1705, 1666, 1592, 1502, 1466, 1434, 1365, 1320, 1233, 1113, 795, 745, 722; ^1H NMR (600 MHz, CDCl_3 , 299K): δ 8.83 (s, 4H, H_{Ar}), 6.50 (s, 4H, H_{Ar}), 4.04 (t, $J = 7.8$ Hz, 4H, $2 \times -\text{OCH}_2$), 3.95 (t, $J = 7.8$ Hz, 8H, $4 \times -\text{OCH}_2$), 1.81-1.26 (m, 96H, alkyl chain), 0.88 (m, 18H, $6 \times -\text{CH}_3$); ^{13}C NMR (150 MHz, CDCl_3 , 298.1K): δ 162.99, 153.79, 138.61, 131.44, 129.36, 127.10, 127.04, 106.70, 73.57, 69.15, 31.98, 31.92, 30.43, 29.80, 29.73, 29.65, 29.60, 29.44, 29.41, 29.36, 29.33, 26.16, 26.11, 22.74, 22.70, 14.15, 14.13. MALDI-TOF mass calculated for $\text{C}_{86}\text{H}_{135}\text{N}_2\text{O}_{10}$ ($\text{M}+\text{H}^+$): 1357.02, found: 1357.841.

Scheme S2. Synthesis of NDI^{10}



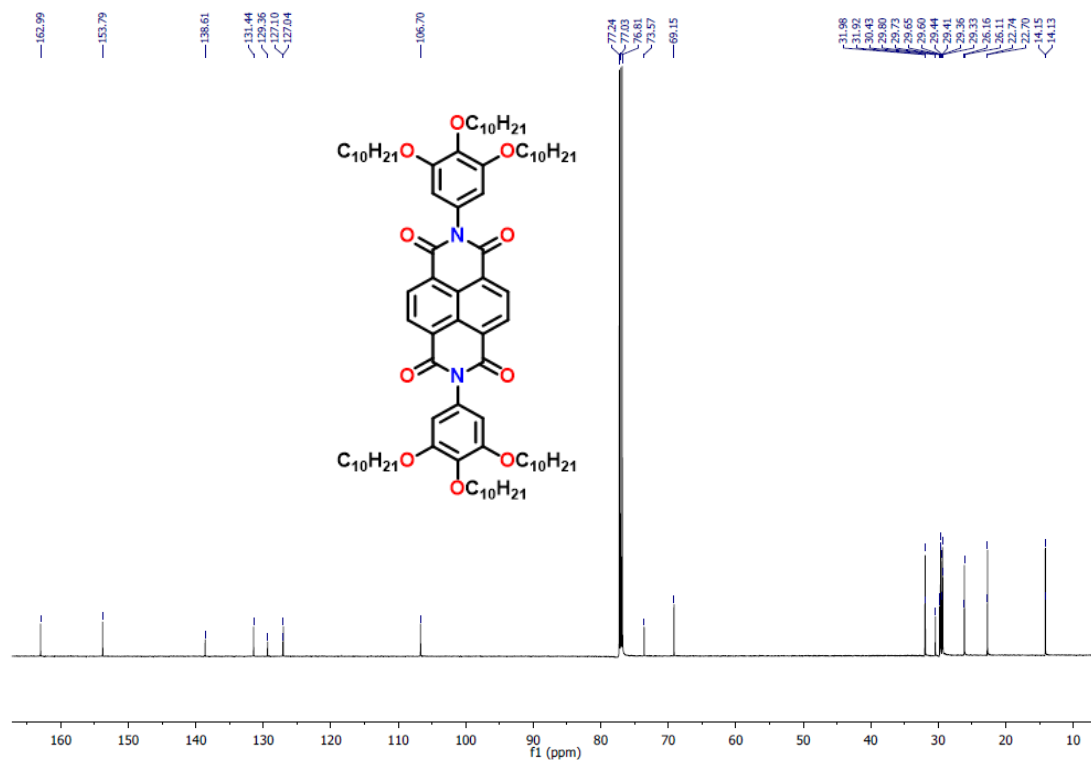
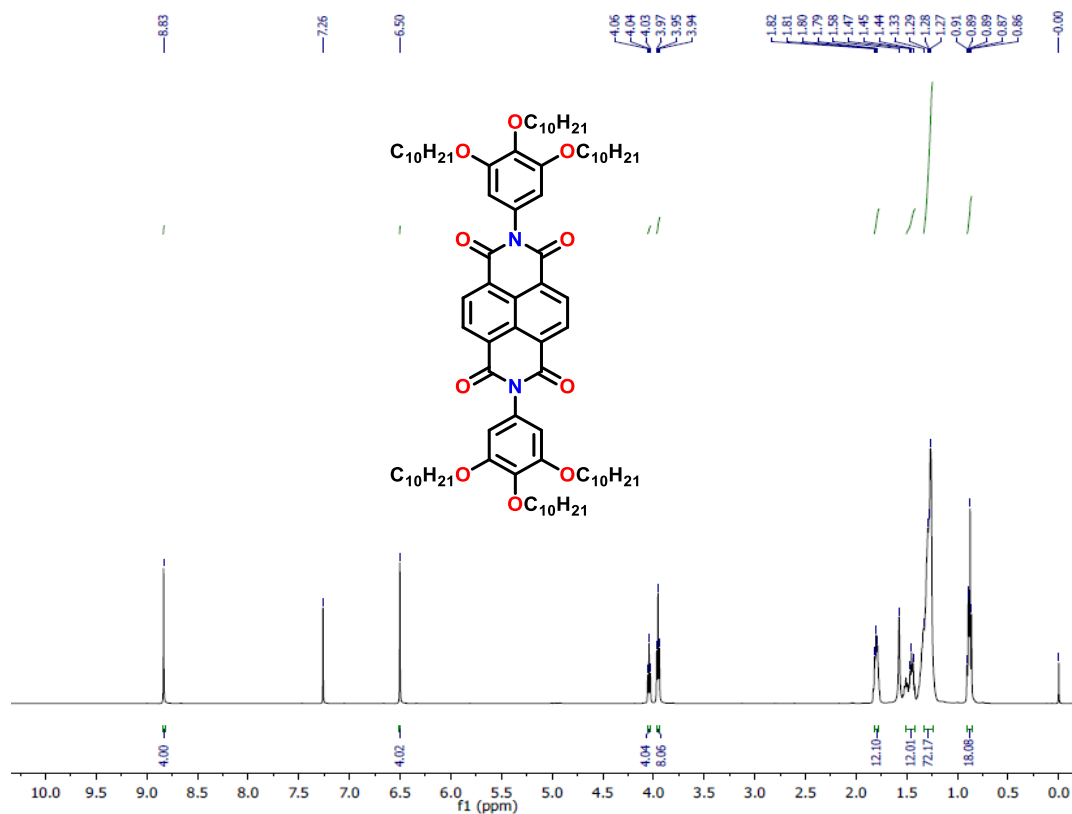
Scheme 2. Reagents and conditions. (i) NaNO_2 , H_2SO_4 , AcOH, H_2O , KI, 90 °C, (91%), (ii) CuI, Et_3N , $\text{Pd}(\text{PPh}_3)_2\text{Cl}_2$, 80 °C, 4 h, (89%), (iii) EtOAc, MeOH, H_2 -Pd/C, rt, overnight (95%), (iv) $\text{Zn}(\text{OAc})_2$, imidazole, microwave irradiation, 35 W, 35 min, 165 °C (86%).

Procedure for synthesis of NDI^{10} [S3]

Naphthalene-3,4,9,10-tetracarboxylic dianhydride (1 eq.), tridecyl aniline (2.2 eq.), zinc acetate (2 eq.) and imidazole (1 g) were taken in a microwave vessel, flushed with nitrogen and put in microwave reactor. The mixture was heated to 165 °C for 35 minutes at 35 W and 100 psi pressure. After cooling, reaction mixture was poured into a 2N HCl (10 mL) solution and extracted with chloroform. Organic layer was washed with water and saturated sodium chloride solution. The crude compound was purified by neutral alumina column chromatography using 50% chloroform-hexane system. Further purification was done by recrystallization from chloroform-methanol system.

NDI¹⁰ : $R_f = 0.6$ (10% EtOAc-Hexane); Off white powdered solid, yield: 86%; IR: ν_{\max} in cm^{-1} : 2922, 2853, 1716, 1674, 1581, 1467, 1348, 1248, 1197, 1119, 980, 878, 819, 767, 743; ^1H NMR (600 MHz, CDCl_3 , 299 K): 8.82 (s, 4H, H_{Ar}), 6.95 (s, 4H, H_{Ar}), 2.65 (t, $J = 7.8$ Hz, 12H, $6 \times -\text{CH}_2$), 1.6 (m, 12H, $6 \times -\text{CH}_2$), 1.5-1.1 (m, 84H, $42 \times -\text{CH}_2$), 0.88 (m, 18H, $6 \times -\text{CH}_3$); ^{13}C NMR (150 MHz, CDCl_3 , 298.1 K): δ 163.41, 142.65, 139.96, 131.92, 131.57, 127.35, 127.33, 126.27, 33.41, 32.22, 32.19, 31.87, 31.52, 30.97, 30.70, 30.23, 29.96, 29.92, 29.88, 29.79, 29.68, 29.63, 29.08, 22.99, 22.96, 22.94, 14.43, 14.41; MALDI-TOF mass calculated for $\text{C}_{86}\text{H}_{135}\text{N}_2\text{O}_4$ ($\text{M}+\text{H}^+$): 1261.04, found: 1261.919.

3. NMR Spectra



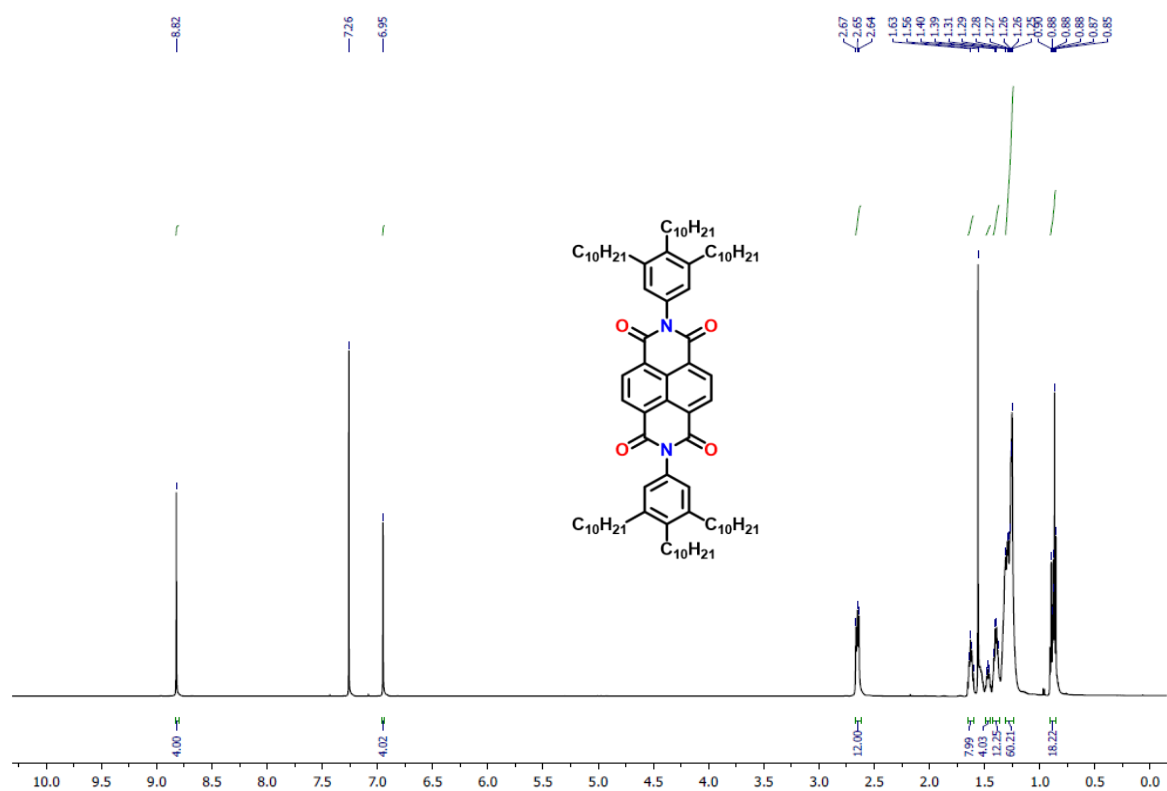


Figure S3. ¹H NMR (600 MHz) spectrum of **NDI¹⁰** in $CDCl_3$.

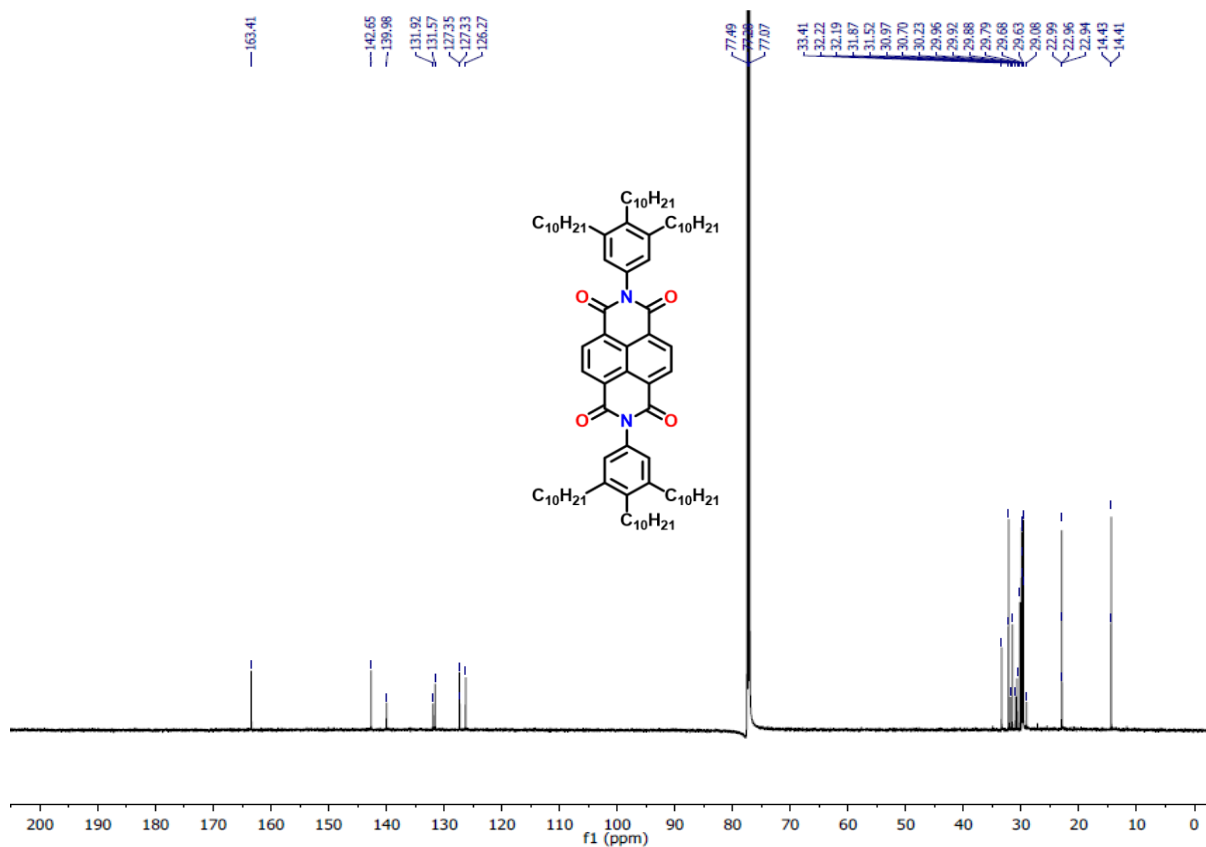


Figure S4. ¹³C NMR (150 MHz) spectrum of **NDI¹⁰** in $CDCl_3$.

4. MALDI-TOF mass spectra

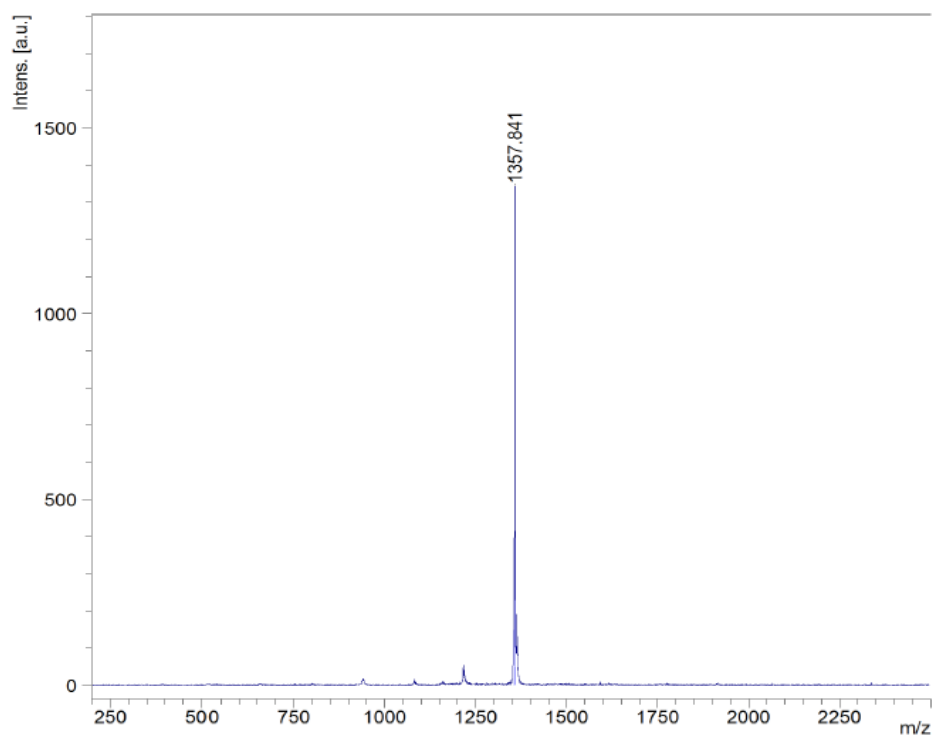


Figure S5. MALDI-TOF mass spectrum of **NDI^{O10}**.

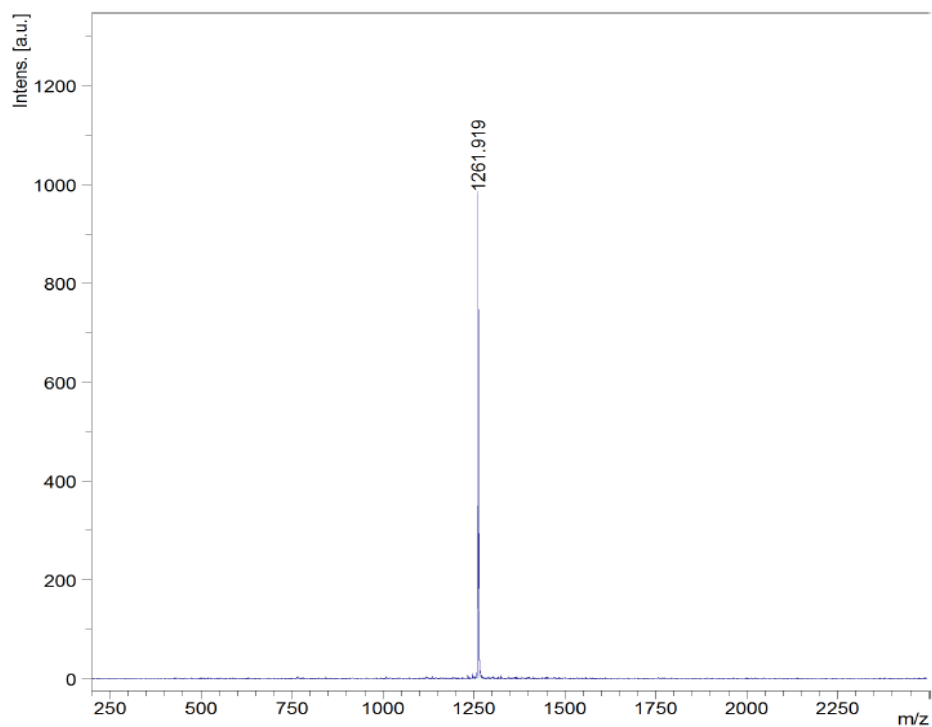


Figure S6. MALDI-TOF mass spectrum of **NDI^{O10}**.

5. Thermal gravimetric analysis (TGA)

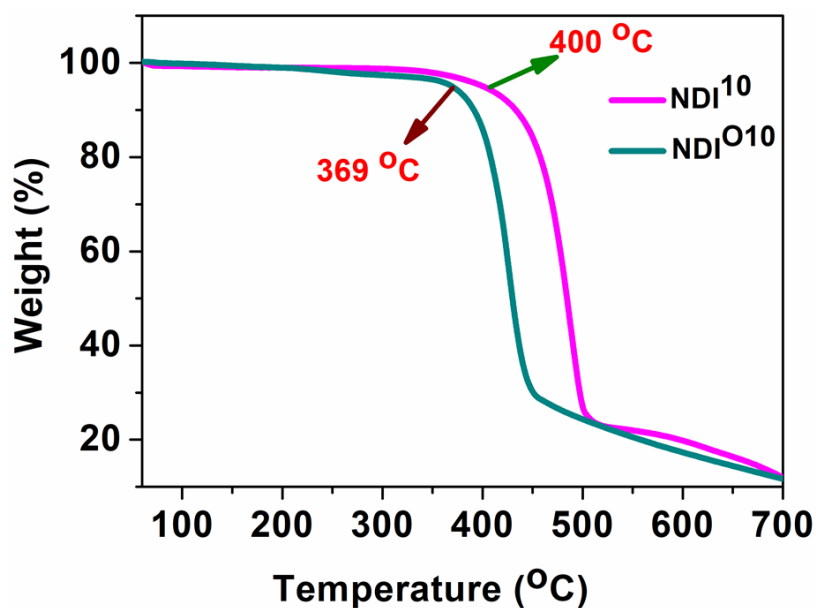


Figure S7. TGA plots of compounds NDI^{O10} and NDI¹⁰ (heating rate of 10 °C/min, Nitrogen atmosphere).

6. Polarizing optical microscopy (POM)

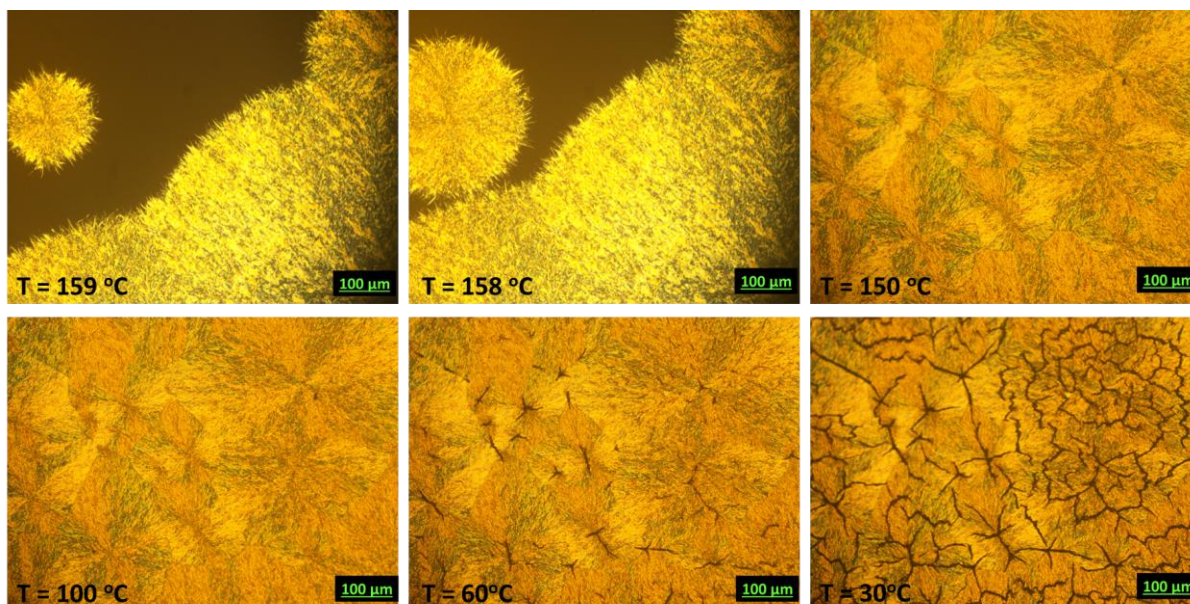


Figure S8. POM images of NDI^{O10} on a cooling process from isotropic melt.

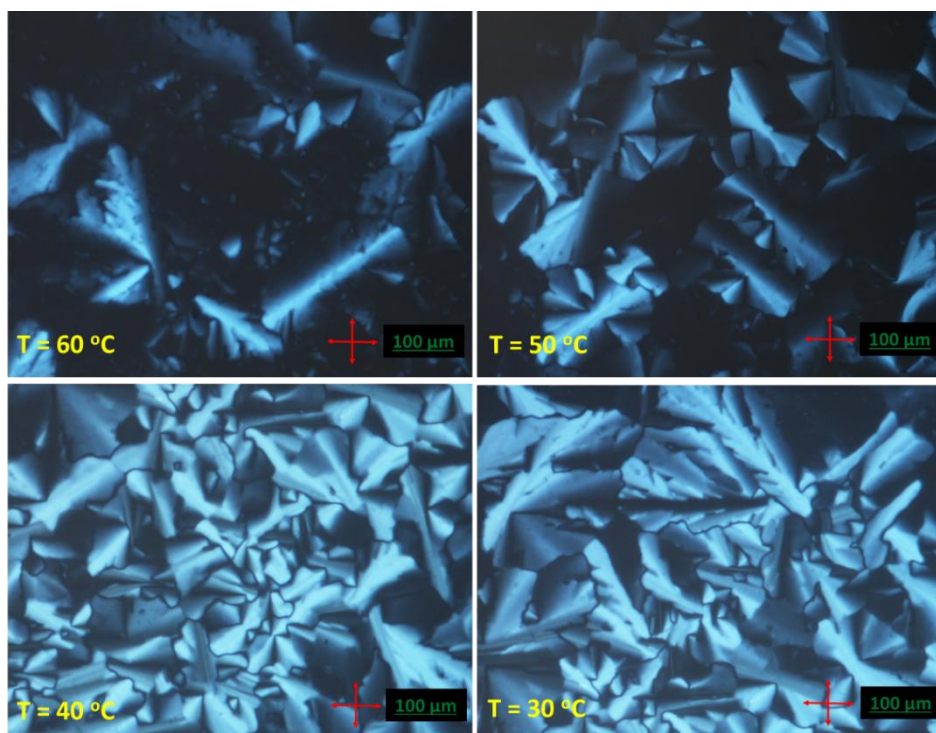


Figure S9. POM images of NDI^{10} on a cooling process from isotropic melt.

7. Differential scanning calorimetry (DSC)

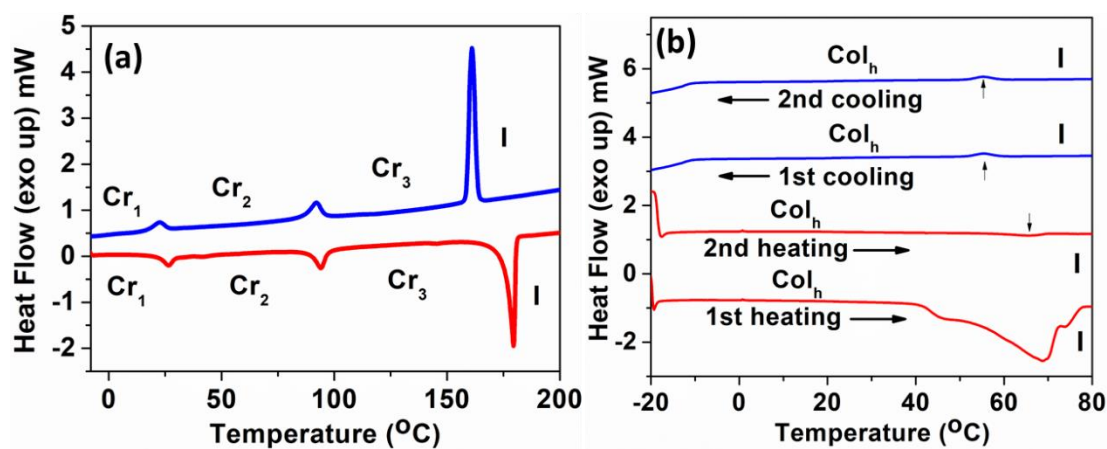


Figure S10. DSC thermograms obtained for NDI^{010} for the first cooling (blue trace) and second heating (red trace) (a) and for NDI^{10} (heating scan: in red trace; cooling scan: in blue trace) (b) taken at $5^\circ\text{C}/\text{min}$.

Table S1. Phase transition temperatures ($^\circ\text{C}$), corresponding enthalpies (kJmol^{-1})^a and decomposition temperatures obtained by TGA.

Compounds	Phase Sequence (kJ/mol)		
	Second heating	First Cooling	Temperature at which 5 wt% decomposition occurred ($^\circ\text{C}$)
NDI^{010}	Cr_1 26.24 (2.48) Cr_2 94.14 (6.15) Cr_3 179.81 (33.10) I	I 161.92 (36.11) Cr_3 92.17 (5.52) Cr_2 22.57 (2.20) Cr_1	369
NDI^{10}	Col_h 65.66 (1.34) I	I 55.36 (1.50) Col_h	400

^a Peak temperatures in the DSC thermograms obtained during the second heating and first cooling cycles at 5°C min^{-1} . Col_h = Columnar hexagonal phase; I = Isotropic phase.

8. X-ray diffraction studies

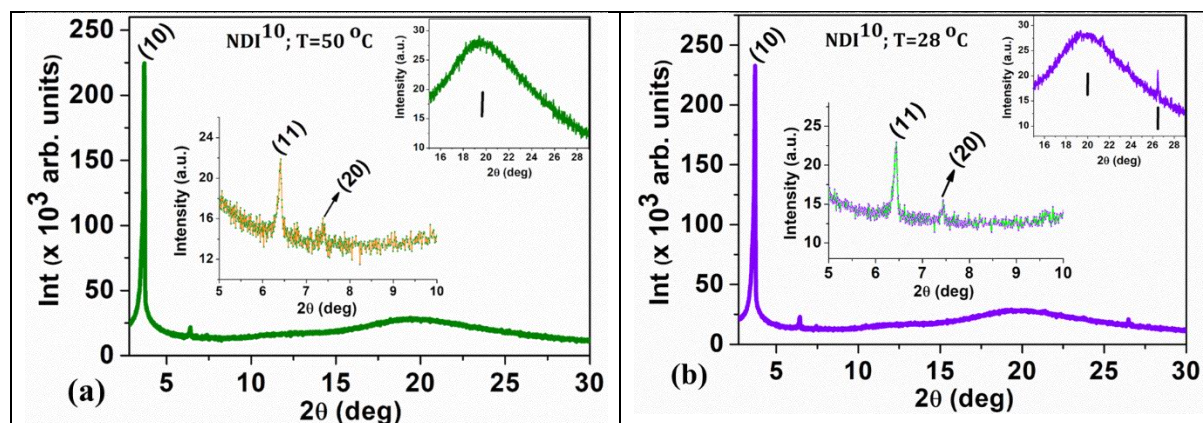


Figure S11. Plot of the intensity against 2θ obtained from the powder XRD pattern of the Col_h phase for compound NDI^{10} at 50 °C (a) and at 28 °C (b).

Table S2. Results of (hkl) indexation of XRD profiles of NDI^{10} at a given temperature (T) of mesophase^a.

Compounds (D/Å)	Phase (T/°C)	d_{obs} (Å)	d_{cal} (Å)	Miller indices (hk)	Lattice parameters (Å), Lattice area S (Å ²), Molecular volume (Å ³)
NDI^{10} (40.92) MW: 1260.03	Col_h (50)	23.96	23.96	10	$a = 27.7, c = 4.52$ $S = 663,$ $V = 2999$ $Z \approx 1$
		13.82	13.83	11	
		11.97	11.98	20	
		7.19 (diffuse)			
		4.52 (h_a)			
	Col_h (28)	23.84	23.84	10	$a = 27.5, c = 4.48$ $S = 656.2$ $V = 2211$ $Z \approx 1$
		13.76	13.76	11	
		11.95	11.92	20	
		6.88 (diffuse)			
		4.48 (h_a)			
		3.37	3.44	44	

^aThe diameter (D) of the disk (estimated from Chem 3D Pro 8.0 molecular model software from Cambridge Soft). d_{obs} : spacing observed; d_{cal} : spacing calculated (deduced from the lattice parameters; a for Col_h phase; c is height of the unit cell). The spacing marked h_a correspond to diffuse reflections in the wide-angle region arising from correlations between the alkyl chains, respectively. Z indicates the number of molecules per columnar slice of thickness h_c (in this case h_a) estimated from the lattice area S and the volume V .

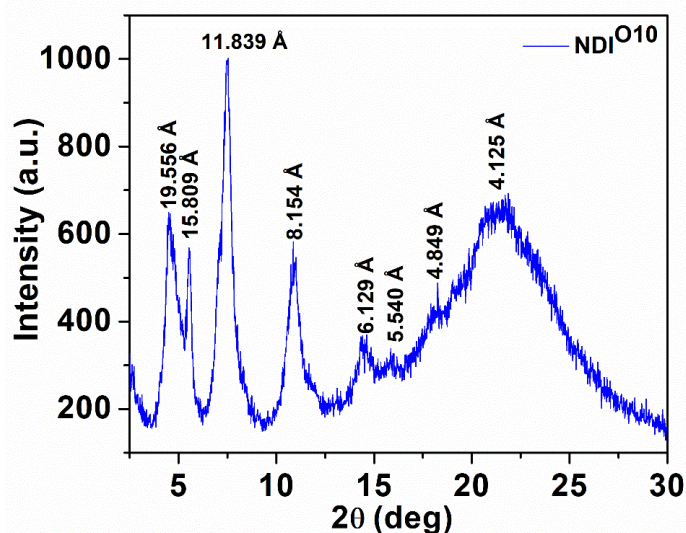


Figure S12. Plot of the intensity against 2θ obtained from the powder XRD pattern of the **NDI^{O10}** at room temperature.

9. Photophysical properties

Table S3. Photophysical properties of **NDI^{O10}** and **NDI^O** in solution^a state.

Entry	Absorption [nm]	Emission ^b [nm]	Stokes Shift (cm ⁻¹)	Molar extinction coefficient (ϵ) (L mol ⁻¹ cm ⁻¹)	$\Delta E_{g, opt}$ ^c [eV]
NDI^{O10}	322, 339, 358, 378	408, 430, 461	3200	26,981	3.16
NDI^O	323, 341, 359, 380	411, 434, 464	3344	23,934	3.15

^a Micromolar solutions in CHCl₃. ^b The excitation wavelength λ_{ex} = 378 and 380 nm respectively, for compounds **NDI^{O10}** and **NDI^O**. ^c Calculated from the red edge of the absorption band.

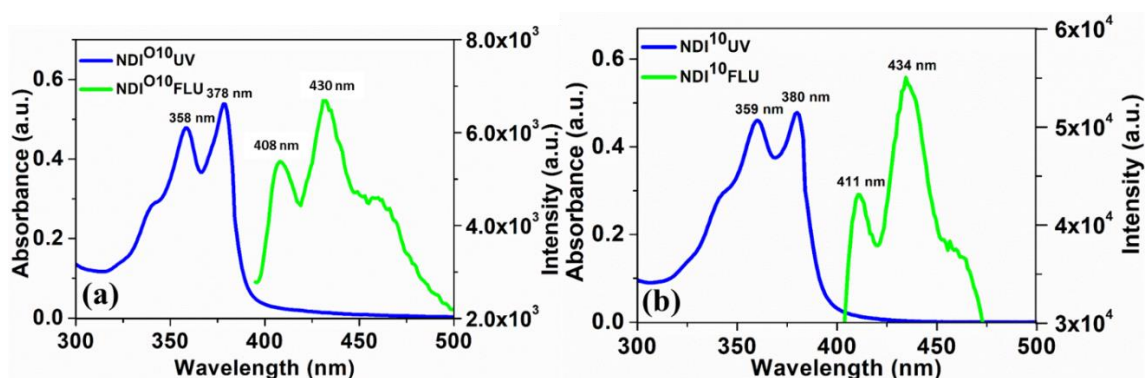


Figure S13. Overlays of absorption spectra (blue trace) and emission spectra (green trace) obtained for compounds **NDI^{O10}** and **NDI^O** in micromolar chloroform solutions.

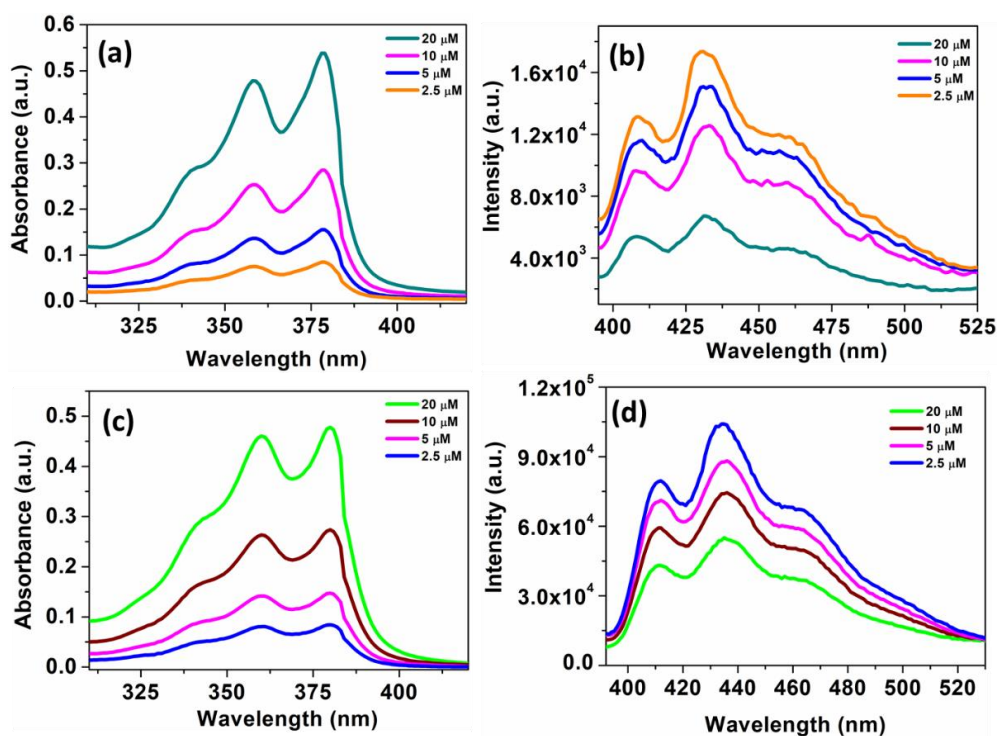


Figure S14. Absorption spectra (a, c) and emission spectra (b, d) of compounds NDI^{O10} and NDI¹⁰ in micromolar chloroform solutions.

10. Electrochemical properties

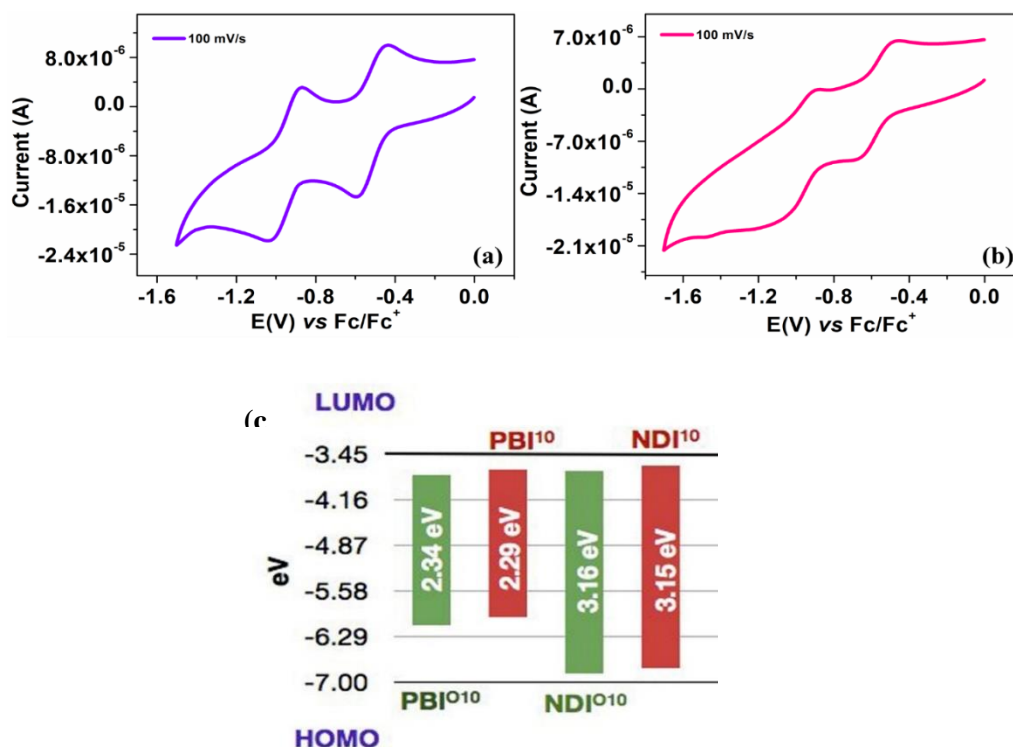


Figure S15. Cyclic voltammograms of NDI^{O10} (a) and NDI¹⁰ (b) in micromolar dichloromethane solutions; (c) Energy band level diagram showing HOMO and LUMO energy levels of corresponding PBIs^{S5b} with the NDIs of present study (from the data obtained from cyclic voltammetry)

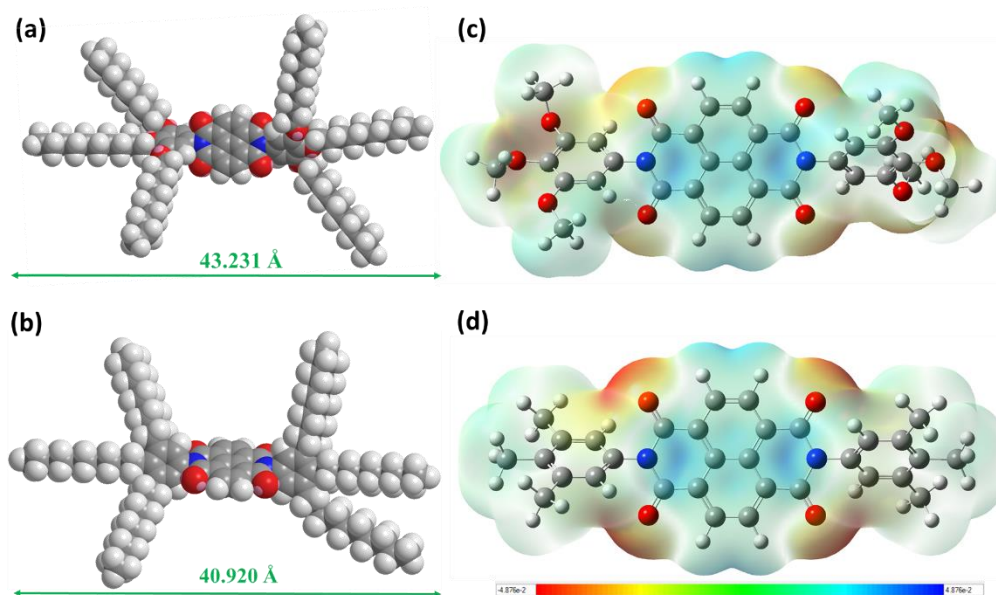
Table S4. Electrochemical^{a,b} data and data obtained from DFT^h calculations for compounds **NDI⁰¹⁰** and **NDI¹⁰**.

Entry	Electrochemical data				Data from DFT calculations		
	E _{1st red} ^[c]	E _{LUMO} ^[d,e]	E _{HOMO} ^[d,f]	ΔE _{g, opt} ^[d,g]	E _{LUMO} ^[d,h]	E _{HOMO} ^[d,h]	ΔE _g ^[d,h]
NDI⁰¹⁰	-0.59	-3.71	-6.87	3.16	-3.95	-5.96	2.01
NDI¹⁰	-0.67	-3.63	-6.78	3.15	-3.79	-6.46	2.67

^[a] 0.5mM Dichloromethane solutions; ^[b]experimental conditions: Ag/AgNO₃ as reference electrode, glassy carbon working electrode, platinum wire counter electrode, TBAP (0.1M) as a supporting electrolyte, room temperature; ^[c] in volts (V); ^[d] in eV; ^[e] estimated from the formula by using E_{LUMO} = -(4.8 - E_{1/2}, Fc/Fc⁺ + E_{red, onset}) eV; ^[f] estimated from the formula E_{HOMO} = E_{LUMO} - E_{g, opt} eV; ^[g]calculated from the red edge of the absorption band of each compound. E_{1/2, Fc/Fc⁺} = 0.50. ^[h] Obtained from DFT calculations by employing the combination of Becke3-Lee-Yang-Parr (B3LYP) hybrid functional and 6-31G(d,p) basis set using the Gaussian 09 package

11. DFT Studies

To understand the electronic properties and frontier molecular orbital energy level of compound **NDI⁰¹⁰** and **NDI¹⁰** computational studies was carried out in B3LYP/6-311g(dp) method using Gaussian 09 program package.^{S6} The absence of imaginary frequency ensured the energy minimized structure of all the compounds.

**Figure S16.** Ground state optimized geometry of **NDI⁰¹⁰** (a) and **NDI¹⁰** (b); molecular electrostatic potential surfaces of **NDI⁰¹⁰** (c) and **NDI¹⁰** (d) (In the mapped electro-static potential surface, the red and blue colors refer to the electron-rich and electron-poor regions, respectively, whereas the green color signifies the zero electrostatic potential, chain length on the phenyl group is limited to methyl for clarity purpose).

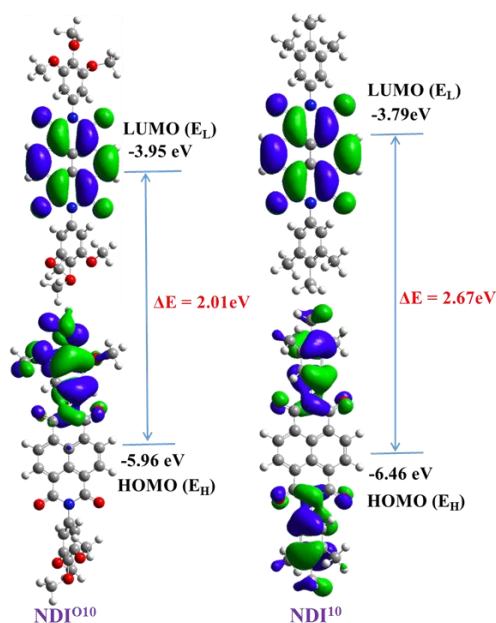


Figure S17. Frontier molecular orbitals of compounds **NDI^{O10}** (a) and **NDI¹⁰** (b) obtained from DFT calculations at the B3LYP/6-31G(dp) level. E_H and E_L denote energies of the highest occupied molecular orbital (HOMO) and the lowest unoccupied molecular orbital (LUMO), respectively.

DFT calculation data for NDI^{O10}:

Center No.	Atomic No.	Atomic Type	Coordinates (Angstroms)		
			X	Y	Z
1	6	0	0.662277	2.311783	0.169529
2	6	0	-0.674610	2.306033	0.165015
3	6	0	-1.356849	1.154427	0.042984
4	6	0	-0.675369	-0.004633	-0.071165
5	6	0	0.684098	0.000552	-0.059604
6	6	0	1.355175	1.165136	0.060600
7	6	0	-1.346374	-1.168877	-0.194669
8	6	0	-0.653328	-2.315299	-0.303926
9	6	0	0.683487	-2.310959	-0.285967
10	6	0	1.365646	-1.159134	-0.166473
11	6	0	2.727867	-1.202645	-0.144818
12	7	0	3.385669	0.010566	-0.036804
13	6	0	2.717250	1.218690	0.064420
14	6	0	-2.719320	1.194889	0.051123
15	7	0	-3.377412	-0.014445	-0.097055
16	6	0	-2.708266	-1.220209	-0.223578
17	8	0	3.351640	-2.242547	-0.179534
18	8	0	3.332458	2.262980	0.118229
19	8	0	-3.343363	2.222376	0.215791
20	8	0	-3.321097	-2.254758	-0.385562
21	6	0	4.745975	0.014943	-0.028075
22	6	0	-4.737556	-0.013782	-0.116510
23	6	0	5.456276	-0.603849	-0.985107
24	6	0	6.800369	-0.592264	-1.014598
25	6	0	7.466623	-0.040157	0.024324
26	6	0	6.794742	0.645170	0.979423
27	6	0	5.448071	0.641262	0.932307
28	6	0	-5.427283	0.798635	-0.930373

29	6	0	-6.770228	0.833402	-0.952079
30	6	0	-7.477727	-0.047405	-0.203499
31	6	0	-6.818854	-0.869919	0.653552
32	6	0	-5.470579	-0.828598	0.659898
33	8	0	7.532277	1.264168	1.964591
34	6	0	6.867805	1.949756	3.000436
35	8	0	8.842088	-0.034504	0.023605
36	6	0	9.416497	-1.132767	0.695194
37	8	0	7.467849	-1.275050	-2.002648
38	6	0	7.852833	-0.466648	-3.091424
39	8	0	-8.850926	0.031516	-0.326682
40	6	0	-9.693595	-0.302999	0.750968
41	8	0	-7.525441	-1.757981	1.430833
42	6	0	-6.863148	-2.834004	2.053830
43	8	0	-7.400390	1.657315	-1.855413
44	6	0	-7.690424	2.938871	-1.343897
45	1	0	1.149617	3.296158	0.269596
46	1	0	-1.170937	3.286134	0.262733
47	1	0	-1.140173	-3.299442	-0.408549
48	1	0	1.179878	-3.291783	-0.376382
49	1	0	4.934312	-1.116385	-1.811332
50	1	0	4.879355	1.138403	1.732651
51	1	0	-4.887949	1.460026	-1.630031
52	1	0	-4.917018	-1.481335	1.351529
53	1	0	7.643404	2.376500	3.675454
54	1	0	6.269703	2.792192	2.586785
55	1	0	6.244274	1.245517	3.595094
56	1	0	10.523411	-1.034548	0.636402
57	1	0	9.106898	-1.132136	1.764026
58	1	0	9.109104	-2.084411	0.207298
59	1	0	8.382022	-1.109092	-3.830086
60	1	0	6.951782	-0.023655	-3.571879
61	1	0	8.541447	0.337820	-2.750358
62	1	0	-10.699651	0.122242	0.534705
63	1	0	-9.821895	-1.404161	0.828562
64	1	0	-9.322164	0.155819	1.694113
65	1	0	-7.639228	-3.486100	2.514059
66	1	0	-6.305790	-3.435414	1.301186
67	1	0	-6.203802	-2.467402	2.871567
68	1	0	-8.202916	3.522914	-2.140558
69	1	0	-8.363784	2.856861	-0.461793
70	1	0	-6.747350	3.457913	-1.060473

DFT calculation data for NDI¹⁰:

Center No.	Atomic No.	Atomic Type	Coordinates (Angstroms)		
			X	Y	Z
1	6	0	0.668701	2.321294	-0.021498
2	6	0	-0.668277	2.321436	-0.016114
3	6	0	-1.356247	1.166760	-0.016283
4	6	0	-0.679740	-0.000743	-0.018323
5	6	0	0.679773	-0.000948	-0.017992
6	6	0	1.356418	1.166436	-0.019440
7	6	0	-1.356356	-1.168247	-0.019887
8	6	0	-0.668694	-2.323064	-0.021646
9	6	0	0.668226	-2.323213	-0.015857
10	6	0	1.356241	-1.168563	-0.015772
11	6	0	2.718539	-1.216374	-0.000890
12	7	0	3.382367	-0.001281	-0.010670

13	6	0	2.718751	1.213850	-0.030163
14	8	0	3.336291	2.256523	-0.088831
15	8	0	3.335435	-2.259624	0.056059
16	6	0	4.742093	-0.001490	0.000508
17	6	0	5.455248	-0.719208	-0.884599
18	6	0	6.800026	-0.733013	-0.887967
19	6	0	7.475888	-0.002915	0.025864
20	6	0	6.783953	0.733379	0.922513
21	6	0	5.439571	0.721091	0.894067
22	6	0	7.482338	1.588185	1.960818
23	6	0	8.992562	-0.019361	0.053867
24	6	0	7.517388	-1.551577	-1.942353
25	6	0	-2.718634	1.214444	-0.001929
26	7	0	-3.382446	-0.000595	-0.013382
27	6	0	-2.718754	-1.215637	-0.031142
28	8	0	-3.336290	-2.258392	-0.088955
29	8	0	-3.335384	2.257671	0.055949
30	6	0	-4.742200	-0.001977	-0.004856
31	6	0	-5.456337	0.719586	-0.885877
32	6	0	-6.801002	0.729926	-0.890087
33	6	0	-7.475877	-0.006935	0.018906
34	6	0	-6.782989	-0.736218	0.920460
35	6	0	-5.438621	-0.720618	0.892789
36	6	0	-7.480045	-1.555293	1.988062
37	6	0	-8.992918	-0.024995	0.018981
38	6	0	-7.519128	1.584281	-1.915153
39	1	0	1.160102	3.308688	-0.023942
40	1	0	-1.159349	3.309073	-0.013543
41	1	0	-1.160091	-3.310591	-0.024229
42	1	0	1.159293	-3.310840	-0.013126
43	1	0	4.924844	-1.298649	-1.658446
44	1	0	4.896581	1.306567	1.654625
45	1	0	8.280206	2.212465	1.499029
46	1	0	6.794037	2.301762	2.466084
47	1	0	7.928128	0.947681	2.755428
48	1	0	9.422712	-0.982639	-0.295528
49	1	0	9.392456	0.797091	-0.589708
50	1	0	9.407339	0.105851	1.077262
51	1	0	6.839535	-1.905381	-2.750764
52	1	0	8.308029	-0.953137	-2.448764
53	1	0	7.976083	-2.457476	-1.484761
54	1	0	-4.927492	1.306002	-1.655630
55	1	0	-4.893766	-1.298956	1.657537
56	1	0	-8.261691	-0.957409	2.508873
57	1	0	-7.946365	-2.461685	1.539268
58	1	0	-6.787017	-1.908284	2.783925
59	1	0	-9.427108	0.102313	-0.996002
60	1	0	-9.415133	-0.989738	0.373890
61	1	0	-9.381576	0.789263	0.672103
62	1	0	-6.840632	2.297487	-2.434225
63	1	0	-7.980634	0.943646	-2.700602
64	1	0	-8.307725	2.208940	-1.438220

12. Charge Carrier Mobility Studies

Charge carrier mobility study of reported NDI based compounds were carried out using Space Charge Limited Current (SCLC) method. A device with ITO/PEDOT: PSS / NDIs /MoO₃/Ag

structure was fabricated for finding the hole mobility whereas ITO/ZnO/ NDIs/Ag was used for finding electron-mobility. In hole and electron only devices ITO/PEDOT: PSS and ITO/ZnO combination was chosen for hole and electron injection. For achieving SCLC regime an Ohmic contact is fundamental requirement with material under test in both hole (Injecting electrode-HOMO) as well as electron (Injecting electrode-LUMO) only devices. Detailed experimental details can be find in the SI section.

In SCLC technique at initial low voltages current follows ohmic with slope of one whereas at higher voltages, where injected charges dominate over intrinsic charges SCLC regime with a slope two is observed. Considering material to be trap free charge mobility of the material can be extracted using Mott-Gurney law given by equation 1

$$J = \frac{9}{8} \varepsilon_0 \varepsilon_r \mu \frac{V^2}{d^3} \quad 1$$

Where ε_0 is the permittivity of free space ($8.86 \times 10^{-14} \text{ F/cm}$), ε_r represents the relative dielectric constant of the material ($\text{NDI}^{010} \sim 3.85$ and $\text{NDI}^{10} \sim 4.87$), V is the applied voltage, d is the thickness of the material and J is density. In thin films where applied electric field is much higher as compared to the bulk, modified Mott–Gurney equation is widely used where a field-dependent charge mobility correction is introduced for the charge mobility calculation shown in equation 2.

$$J = \frac{9}{8} \varepsilon_r \varepsilon_0 \mu \frac{V^2}{d^3} \exp\left(0.891\gamma \sqrt{\frac{V}{d}}\right) \quad 2$$

where γ is the fitting parameter that represents the strength of the field dependence of mobility. In this work modified Mott-Gurney equation was used for fitting the measured $J-V$ curves for both NDIs to extract hole and electron mobilities. Electron and hole mobility values for both NDIs is summarized in Table S5. Figures 4a,b represent the observed as well as SCLC fitted curves for both NDIs respectively. The reported mobility values for both electron and hole are an average of at least 5 devices (Table S5).

Table S5. Hole and electron mobility values for both NDIs

Entry	NDI¹⁰	NDI⁰¹⁰
Hole mobility (cm ² / V.s)	1.49E-03 2.67E-03 2.84E-03 2.57E-03 2.47E-03	2.77E-03 3.28E-03 2.22E-03 2.90E-03 1.83E-03
Avg. Stdev	2.41E-03 4.74E-04	2.60E-03 5.14E-04
Electron mobility (cm ² / V.s)	1.02E-03 1.05E-03 1.13E-03 1.16E-03 1.01E-03	2.52E-03 2.98E-03 2.08E-03 1.94E-03 1.53E-03
Avg. Stdev	1.07E-03 6.02E-05	2.21E-03 4.98E-04

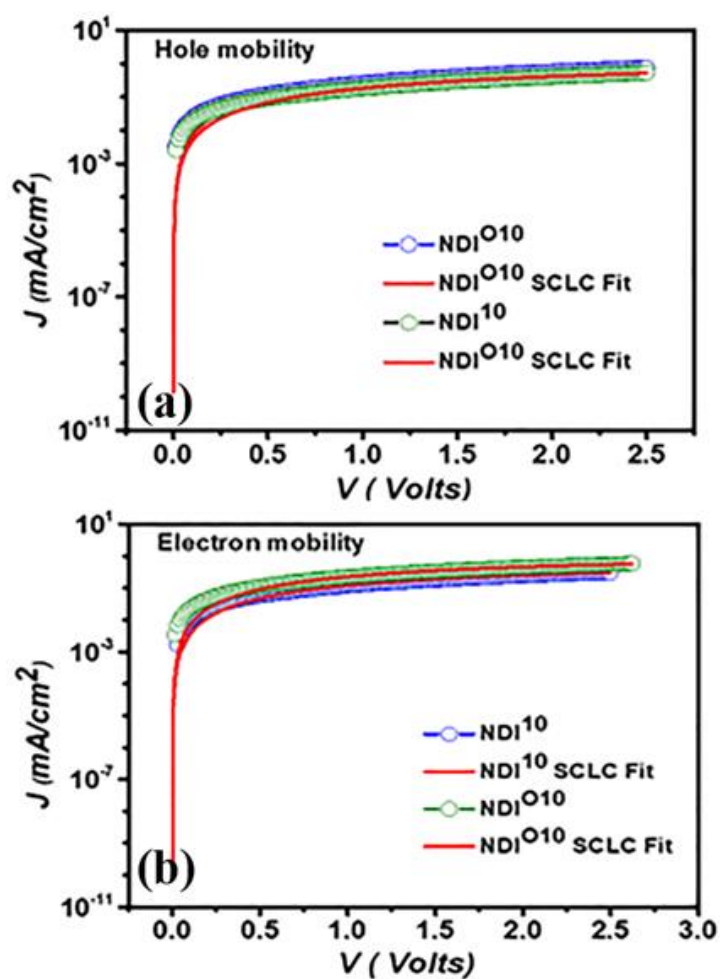


Figure S18. J-V curves along with SCLC fitting for NDIs on semi log scale (a) for hole mobility; (b) for electron mobility

13. References

- S1. C. V. Yelamaggad, A. S. Achalkumar, D. S. S. Rao, and S. K. Prasad; *J. Org. Chem.* **2007**, 72, 8308-8318
- S2. V. Percec, M. Peterca, T. Tadjiev, X. Zeng, G. Ungar, P. Leowanawat, E. Aqad, M. R. Imam, B. M. Rosen, U. Akbey, R. Graf, S. Sekharan, D. Sebastiani, H. W. Spiess, P. A. Heiney, and S. D. Hudson; *J. Am. Chem. Soc.* **2011**, 133, 12197–12219.
- S3. R. K. Gupta, D. S. S. Rao, S. Krishna Prasad, and A. S. Achalkumar; *Chem. Eur. J.* **2018**, 24, 3566 – 3575.
- S4. X. Zhang, Z. Chen, and F. Würthner; *J. Am. Chem. Soc.* **2007**, 129, 4886-4887.

S5. (a) Z. Chen, V. Stepanenko, V. Dehm, P. Prins, L. D. A. Siebbeles, J. Seibt, P. Marquetand, V. Engel, and F. Wurthner; *Chem. Eur. J.* **2007**, *13*, 436 – 449. (b) P. K. Behera, M. R. Nagar, R. K. Gupta, S. Pradhan, D. S. S. Rao, S. K. Prasad, L. The, A. Choudhury, J.-H. Jou and A. S. Achalkumar, *J. Mater. Chem. C*, **2022**, *J. Mater. Chem. C*, 2022, 10, 18351-18365.

S6. a) Gaussian 09, Revision B.01, M. J. Frisch, G. W. Trucks, H. B. Schlegel, G. E. Scuseria, M. A. Robb, J. R. Cheeseman, G. Scalmani, V. Barone, B. Mennucci, G. A. Petersson, H. Nakatsuji, M. Caricato, X. Li, H. P. Hratchian, A. F. Izmaylov, J. Bloino, G. Zheng, J. L. Sonnenberg, M. Hada, M. Ehara, K. Toyota, R. Fukuda, J. Hasegawa, M. Ishida, T. Nakajima, Y. Honda, O. Kitao, H. Nakai, T. Vreven, J. J. A. Montgomery, J. E. Peralta, F. Ogliaro, M. Bearpark, J. J. Heyd, E. Brothers, K. N. Kudin, V. N. Staroverov, R. Kobayashi, J. Normand, K. Raghavachari, A. Rendell, J. C. Burant, S. S. Iyengar, J. Tomasi, M. Cossi, N. Rega, J. M. Millam, M. Klene, J. E. Knox, J. B. Cross, V. Bakken, C. Adamo, J. Jaramillo, R. Gomperts, R. E. Stratmann, O. Yazyev, A. J. Austin, R. Cammi, C. Pomelli, J. W. Ochterski, R. L. Martin, K. Morokuma, V. G. Zakrzewski, G. A. Voth, P. Salvador, J. J. Dannenberg, S. Dapprich, A. D. Daniels, O. Farkas, J. B. Foresman, J. V. Ortiz and J. Cioslowski Fox, *D. J. Gaussian Inc., Wallingford, CT*, **2009**; b) C. Lee, W. Yang and R. G. Parr, *Phys. Rev. B*, **1988**, *37*, 785–789; c) A. D. Becke, *J. Chem. Phys.*, **1993**, *98*, 1372–1377.